

A Numerical Study on Performance of Air-to-Air Plastic Plate Heat Exchanger

Minho Chung, Seongyeon Yoo^{†*}, Kyuhyun Han^{*}, Hongik Yoon^{**}, Hyoungchul Kang^{**}

Technology Research Institute, Daelim Industrial Co. Ltd., Seoul, Korea 110-732

**BK21 Mechatronics Group, Chungnam National University, Daejeon, Korea 305-764*

***Gagyo Tech Co., Ltd, Daejeon, Korea 305-333*

(Received March 2, 2009; Revision received May 21, 2009; Accepted June 5, 2009)

Abstract

The purpose of this research is to develop high efficiency plastic plate heat exchangers which can be substituted for conventional aluminum plate heat exchangers. Four simulation models of plastic plate heat exchangers are designed and simulated: that is, flat plate type, turbulent promoter type, corrugate type and dimple type heat exchanger. The flat plate type is designed as the reference model in order to evaluate how much thermal performance increases. The turbulent promoter type is fabricated with cylindrical-type vortex generators and rib-type turbulent promoters. The corrugate type is obtained from the conventional stainless steel compact heat exchangers, which are called the herringbone-type compact heat exchangers. The dimple type has a number of dimples on its surface. In this study, the flow and heat transfer characteristics of the plastic plate heat exchanger are investigated using numerical simulation and compared with experimental results. Numerical simulation is carried out using the FLUENT code. The flows are assumed as a three-dimensional, incompressible and turbulent model. The computational analysis and experimental results both show that the friction coefficient and Nu number is highest in the corrugate type. The tendency of numerical simulation results is in good agreement with that of the experimental results.

Key words: Plastic plate heat exchanger, Numerical simulation, Exhaust heat recovery

Nomenclature

c : Heat capacity [J/kg K]
 f : Friction factor
 g : Gravitational acceleration [m/s^2]
 h : Heat transfer coefficient [$W/m^2 K$]
 k : Turbulent kinetic energy [J]
 Nu : Nusselt number
 p : Pressure [Pa]
 Pr : Prandtl number
 q : Heat flux [W/m^2]
 Re : Reynolds number
 T : Temperature [K]
 T_{wall} : Wall temperature [K]
 T_{ref} : Reference temperature [K]
 $T.I.$: Turbulence Intensity
 U : Mean velocity of component [m/s]
 u : Fluctuating velocity of component [m/s]

Greek symbol

α : Thermal diffusivity [m^2/s]
 β : Coefficient of thermal expansion [K^{-1}]
 ε : Turbulent dissipation rate [m^2/s^3]
 ν : Kinematic viscosity [m^2/s]
 ρ : Density [kg/m^3]
 σ : Turbulent Prandtl number

1. Introduction

With the current trend towards airtight and insulated indoor living spaces along with the distribution and improvement of air-conditioning and heating equipment, people tend to stay longer indoors with the windows closed. This has resulted in absolute lack of ventilation and posed problems such as air quality deterioration by harmful substances emitted from construction materials and household care products. The key to handling this is the inflow of fresh air

[†]Corresponding author. Tel.: +82 42 821 6646, Fax.: +82 42 821 8036
E-mail address: syyooh@cnu.ac.kr

from outside. However, the inflow of cold outdoor air in winter inevitably leads to costly heating energy consumption. In much the same way, the inflow of hot external air in summer results in increased air-conditioning load and enormous energy loss. As a means to solve these problems, it is necessary to install an appropriate ventilation system and develop an exhaust heat recovery system utilizing heat exchange between supplied air (outdoor air) and exhaust air (indoor air). The installation of an exhaust heat recovery heat exchanger enables the recovery 50 ~ 70% of exhaust heat and thus saves heating energy in winter and air-conditioning energy in summer. Exhaust heat recovery heat exchangers are available in various types: aluminum plate, rotary, heat pipe and thermosiphon. These heat exchangers are hard to maintain and expensive, so they are usually found only in commercial buildings. The aluminum plate heat exchangers have been used widely for ventilation heat recovery in the air-conditioning system, and various nonmetallic materials such as pulp, teflon, and plastic have been adopted as a material of heat exchangers for the same usage. Among those nonmetallic materials, plastic is one of the most promised materials because of its competitive mechanical advantages: low cost, light weight, easy processing, high corrosion-resistance, and so on (1). The principal aim of this research is to find high efficiency plastic plate heat exchangers which can be substituted for aluminum plate heat exchangers.

Fiebig et al. (2) attached a vortex generator between plates using fins so as to enhance the heat transfer of an air-to-air plate heat exchanger. While changing the angle, number and size of the vortex generator, they conducted a numerical-analytic investigation of these variables' influence on heat transfer characteristics and pressure loss, and proposed improvements of the design of the plate heat exchanger using a vortex generator. In order to analyze the convective heat transfer of a heat exchanger with manipulated fin surface, Choi et al. (3) conducted a computational analysis of the flow field and temperature field of a 2D channel flow with dimples on one side. Results showed that within the dimples is a vortex which is moved toward the downstream side, suggesting that heat transfer is most enhanced near the downstream edge of the dimple. It was also found that a channel flow with a dimple always has a lower pressure loss than a fully developed 2D flat plate channel flow. Stasiek (4) measured overall & local

heat transfer coefficients and pressure loss distribution at various Reynolds numbers and angles using liquid crystals on a corrugate heat exchanger surface. Yoo et al. (5) conducted performance tests on 5 types of plastic plate heat exchangers (flat plate type, plate fin type, turbulent promoter type, corrugate type and dimple type). As a result of comparing their actual performances taking heat transfer performance and pressure loss into consideration, it was found that the performances of the corrugate type, turbulent promoter type and dimple type at the wind velocity of 2.5m/s were increased by 43%, 14 and 33% respectively and that the higher the wind velocity, the higher the performance.

In this study, a computational analysis was conducted to develop a plastic plate heat exchanger for exhaust heat recovery system, which is much cheaper and has much higher heat performance than the existing aluminum plate heat exchanger. The analysis was aimed at understanding the complex flow field and local heat transfer inside the flat plate heat exchanger and presenting basic data for a flat plate heat exchanger design. It was conducted using FLUENT, a commercial computational fluid dynamics code, on four models including; a flat plate type designed as a reference model, a turbulent promoter type using a vortex generator and a turbulent promoter, a corrugate type used for industrial metal plate heat exchanger, and a dimple type using hemispherical asperity-shaped dimples. The computational results were compared with those experimental results obtained Yoo (5).

2. Governing equations and boundary conditions

The governing equations for analysis of the flow and heat transfer of a plastic plate heat exchanger are as follows.

- Continuity Equation

$$\frac{\partial U_i}{\partial x_i} = 0 \quad (1)$$

- Momentum Equation

$$U_k \frac{\partial U_i}{\partial x_k} = -\frac{1}{\rho} \frac{\partial p}{\partial x_i} + \frac{\partial}{\partial x_k} \left(\nu \frac{\partial U_i}{\partial x_k} - u_i u_k \right) \quad (2)$$

○ Energy Equation

$$U_k \frac{\partial T}{\partial x_k} = \frac{\partial}{\partial x_k} \left(\alpha \frac{\partial T}{\partial x_k} - u_k \theta \right) + \frac{\dot{q}}{\rho c} \quad (3)$$

The standard k-ε model is used as the turbulent flow modeling. The equations concerning the turbulence kinetic energy k and the turbulence dissipation rate ε are written as follows.

$$U_k \frac{\partial k}{\partial x_k} = \frac{\partial}{\partial x_k} \left[\left(\nu + \frac{\nu_t}{\sigma_k} \right) \frac{\partial k}{\partial x_k} \right] + G_k + G_b - \varepsilon \quad (4)$$

$$U_k \frac{\partial \varepsilon}{\partial x_k} = \frac{\partial}{\partial x_k} \left[\left(\nu + \frac{\nu_t}{\sigma_\varepsilon} \right) \frac{\partial \varepsilon}{\partial x_k} \right] + \frac{\varepsilon}{k} (C_1(G_k + G_b) - C_2) \quad (5)$$

$$G_k = \nu_t \left(\frac{\partial U_i}{\partial x_i} + \frac{\partial U_i}{\partial x_j} \right) \frac{\partial U_j}{\partial x_i}, \quad G_b = \beta g_i \frac{\nu_t}{Pr} \frac{\partial T}{\partial x_i},$$

$$\nu_t = C_\mu \frac{k^2}{\varepsilon}, \quad C_1 = 1.44, \quad C_2 = 1.92,$$

$$C_\mu = 0.09, \quad \sigma_k = 1.0, \quad \sigma_\varepsilon = 1.3$$

The computational analysis was conducted under the assumption that cold air is drawn into the inlet of each plastic plate heat exchanger and the upper and lower heat exchanger plates are maintained at a higher temperature than the air temperature at the inlet. The velocities and temperature conditions at the inlet and plate surface of the plastic plate heat exchanger are as follows.

○ Boundary conditions at the inlet

$$U = 1.0, 2.5, 5.0 \text{ m/s}, \quad T = 10^\circ\text{C}, \quad T.I. = 1\%$$

○ Boundary conditions at the plate surface

$$U = 0.0 \text{ m/s}, \quad T = 50^\circ\text{C}$$

3. Computational analysis methodology

The governing equations and turbulent equations are written in a general form as follows.

$$\frac{\partial}{\partial x_k} (\rho U_k \phi) = \frac{\partial}{\partial x_k} \left(\Gamma_\phi \frac{\partial \phi}{\partial x_k} \right) + S_\phi \quad (6)$$

The left-hand side term is a convection term, the first term of the right-hand side term is a diffusion term,

and S_ϕ is a source term. $\phi = 1$ indicates a continuity equation, $\phi = U_i$ indicates a momentum equation, $\phi = T$ indicates an energy equation, and $\phi = k, \varepsilon$ indicates a turbulent equation. The source term is expressed in a different form for each governing equation. The difference equation for the governing equation (6) for control volume can be obtained by using a FVM (Finite Volume Method) and is written as follows.

$$\phi_p \sum_i (A_i - S_p) = \sum_i (A_i \phi_i) + S_c \quad (7)$$

FLUENT, a commercial thermo-fluid analysis program, was used to obtain the solution of the difference equation (7). It is a program developed for numerical analysis concerning flow, heat transfer, phase change, combustion etc. and composed of GAMBIT (preprocessor), FLUENT (solver and postprocessor). A FVM code using a fully implicit scheme, FLUENT uses non-staggered grids which store vector quantities (velocity etc.) and scalar quantities (pressure, temperature etc.) in the same place. The interpolation between the grid points for computation of the convection term can be used with either the power-law method, the 2nd order upwind difference method or the QUICK method (high order upwind difference method). The turbulent model basically uses a k-ε model and can selectively use either the RSM (Reynolds Stress Model) or the RNG (Renormalization Group). The numerical solution employs SIMPLE and SMMPLEC (6). In this study, the computational analysis was conducted using a first order upwind scheme, a k-ε turbulent model and a SIMPLE algorithm. A convergence test for each model was performed at the time the total of the following whole-range remnant terms falls below.

$$\bar{R} = \frac{\sum_{nodesP} \left[A_E \phi_E + A_W \phi_W + A_N \phi_N + A_S \phi_S + S_c - A_P \phi_P \right]}{\sum_{nodesP} \left[A_P \phi_P \right]} \leq 10^{-6} \quad (8)$$

4. Heat exchanger modeling

Grids were created for each of four types of plastic plate heat exchanger models and then a computational analysis was performed to compare and examine the results. The one used as a reference model is the flat plate type heat exchanger, with a 160×160 mm heat transfer surface and a 4 mm gap between the plates. Fig. 1 shows the schematic and grid of heat exchanger

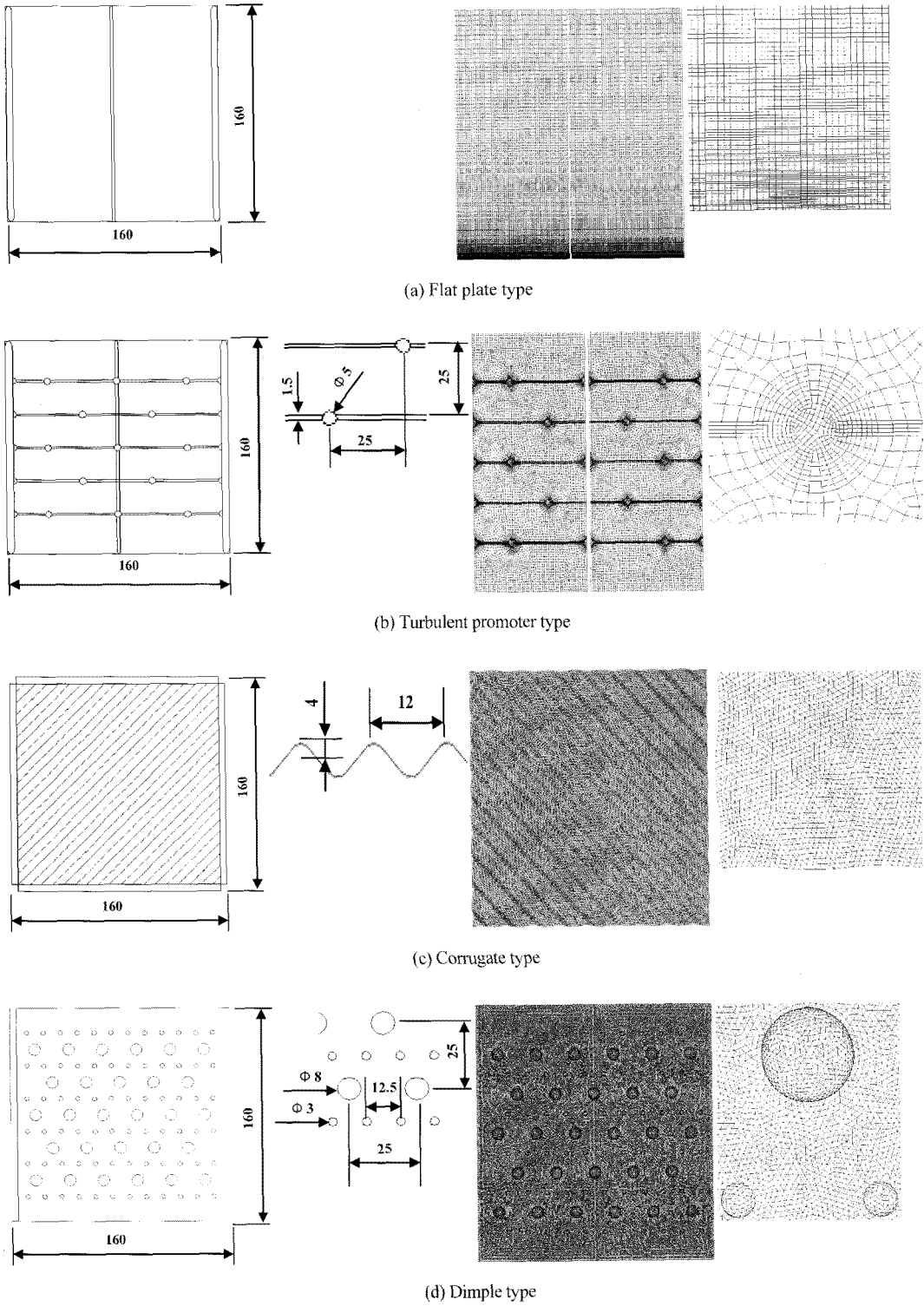


Fig. 1. Schematic and grid of plastic plate heat exchanger.

models. As illustrated in Fig. 1(a), grids were densely distributed near the inlet of the flow where a boundary layer begins to develop and on the upper and lower plates where a thermal boundary layer forms. The second model is the turbulence promoter type heat exchanger where a 5 mm diameter cylindrical-type vortex generator and a 1.5×1.5 mm rib-type turbulence promoter are installed perpendicularly to the flow direction and crosswise on the upper and lower plates respectively. As shown in Fig. 1(b), this model was modeled by densely distributing grids near the vortex generator and the turbulence promoter where the flow changes rapidly. The third model is the corrugate type heat exchanger with corrugated plates, which was modeled after a herringbone type heat exchanger used for the existing industrial metal plate heat exchanger. For the most efficient heat transfer, plates were conjoined at the angle of 90° with a 12 mm wave length and height of wave is a 4 mm. Since the shapes of the flow channel and the heat transfer surface is very complicated, the corrugate type was modeled using tetrahedral grids. Fig. 1(c) shows the corrugate heat exchanger grids. The first and second models were modeled using about 200,000 grids

while the corrugate type was modeled using about 1,200,000 grids. The fourth model is the dimple type heat exchanger with 8 and 3 mm diameter hemispherical dimples placed crosswise at a gap of 25 mm. Since the upper and lower plates are arranged crosswise, a very complicated channel flow is formed. Because it shows a very complicated flow in which a vortex is formed in front of the hemispherical dimples and the second flow is formed within the dimples, a total of 1,800,000 tetrahedral grids were used to develop the computational model shown in Fig. 1(d). Computations were conducted at the inlet flow of 1 m/s, 2.5 m/s, 5 m/s under the assumption that the cold air (10 °C) is drawn into the inlet and the upper and lower plates are continuously maintained at 50 °C.

5. Results and discussions

Fig. 2(a) shows the velocity distribution inside the flat plate type heat exchanger. The air flow is exiting the outlet along the flat plate in a uniform distribution and the velocity is a little low due to the wall surface at both ends of the flat plates. Fig. 2(b) shows the velocity distribution of the turbulent promoter type

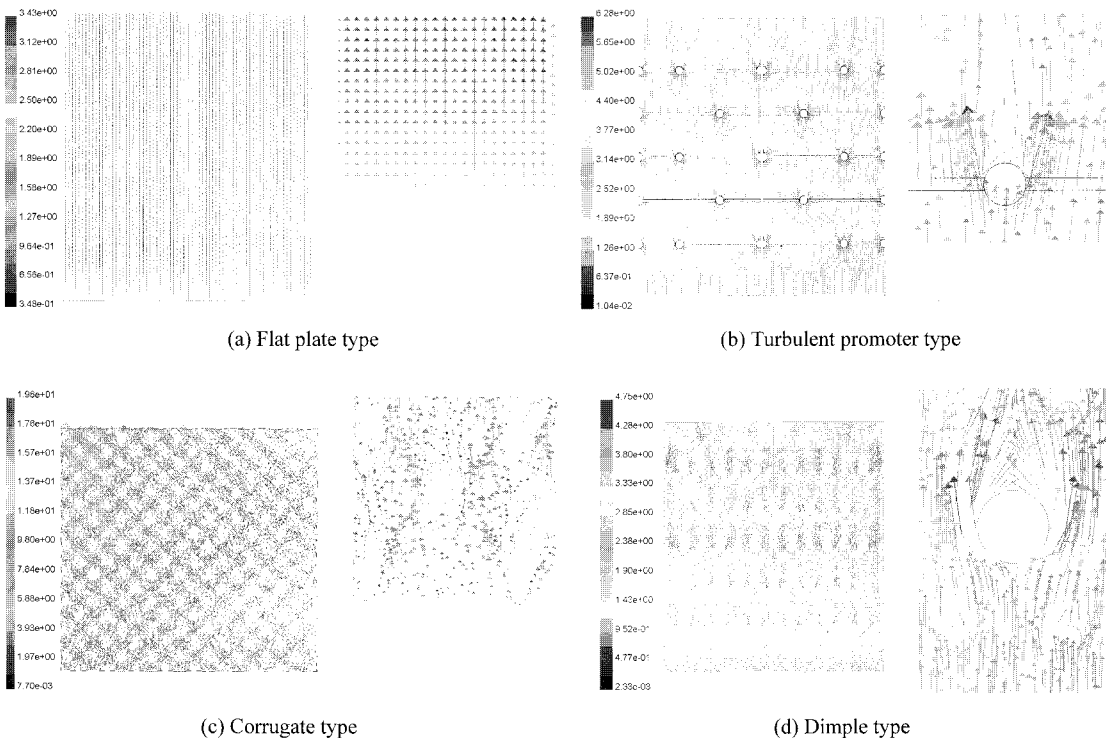


Fig. 2. Velocity distribution of plastic plate heat exchanger.

heat exchanger: the air drawn into the inlet forms a stagnation point in the cylindrical vortex generator in the first row, flows along the circular pipe and accelerates by a favorable pressure gradient. The flow passing through the middle of the circular pipe decelerates due to an adverse pressure gradient and finally there occurs a separation phenomenon at around 120° behind the circular pipe from the stagnation point, forming a separation zone behind the circular pipe. The recirculation zone extends to the turbulent promoter in the second row, this phenomenon occurs at every cylindrical vortex generator. Where a square bar turbulent promoter is installed, the flow area decreases rapidly and the flow boundary layer is destroyed, showing a high velocity distribution. Fig. 2(c) shows the velocity distribution inside the corrugate type heat exchanger. The air drawn into the inlet circulates in a complicated flow along the valleys of the lower plate and the peaks of the upper plates. The flow moving along the valleys changes its direction by 90° when it reaches the sidewall. Fig. 2(d) shows the velocity distribution inside the dimple type heat exchanger. As in the vortex generator of the turbulent promoter type heat exchanger, the air accelerates

beside the dimple and there occurs a recirculation zone behind the dimple.

Fig. 3 shows the local heat transfer coefficient distribution for the plastic plate heat exchangers. The heat transfer coefficient is written as follows.

$$h = \frac{\dot{q}}{(T_{wall} - T_{ref})} \tag{9}$$

where the T_{wall} is the wall temperature, T_{ref} is the reference temperature. In this study, the reference temperature uses the average temperature between the inlet and the surface temperature of the plastic plate heat exchanger. Fig. 3(a) shows the local heat transfer coefficient distribution on the heat transfer surface of the flat plate type heat exchanger. The heat transfer coefficient is highest at the inlet, decreases rapidly from the inlet and maintains a constant value as it approaches the fully developed flow. The decrease of the heat transfer coefficient decreases from the inlet is because the heat boundary layer gets thicker as the flow progresses. Fig. 3(b) shows the heat transfer coefficient distribution of the turbulent promoter type heat exchanger. When the boundary layer flow

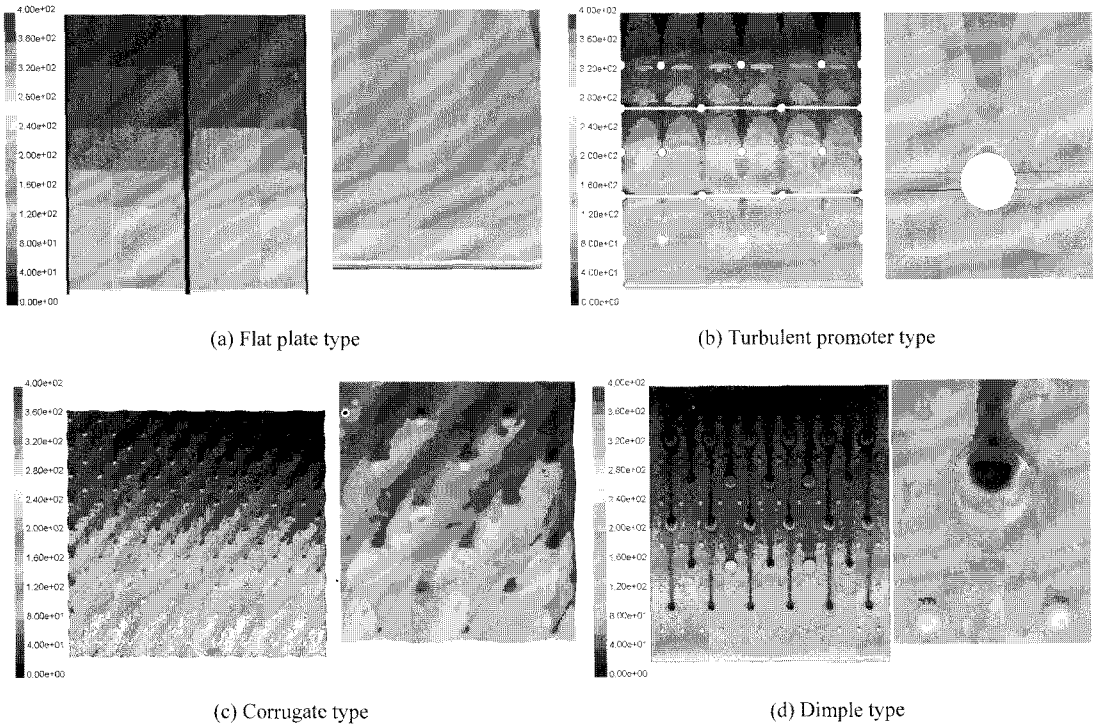


Fig. 3. Distribution of local heat transfer coefficient for plastic plate heat exchanger.

reaches the cylindrical vortex generator, dynamic pressure turns into static pressure and a pressure gradient is formed. This pressure gradient causes a flow towards the plates. When reaching the plates, the flow turns into a back flow and forms a horseshoe vortex. As the horseshoe vortex along with the main flow progresses around the turbulent promoter, heat transfer is promoted. In front of and around the vortex generator appears a zone where heat transfer is promoted by the horseshoe vortex. Meanwhile, since the flow area decreases where the turbulent promoter is installed, velocity increases destroying the thermal boundary layer and forming a new thermal boundary layer resulting in a high heat transfer coefficient over a very wide range. Fig. 3(c) shows the heat transfer coefficient distribution of the corrugate type heat exchanger. A high heat transfer coefficient distribution is shown at the flow inlet. It decreases as the flow develops towards the outlet. A high heat transfer coefficient is found in the decreased flow area where the peaks of the lower plate and the valleys of the upper plate meet. A relatively high heat transfer coefficient is shown along the peaks with a small flow area while a low heat transfer coefficient is shown along the valleys with a large flow area. Fig. 3(d) shows the heat transfer coefficient distribution of the dimple type heat exchanger. As in other heat exchangers, the heat transfer coefficient is highest at the inlet. The heat transfer coefficient is high due to the influence of the horseshoe vortex in front of the 3 mm dimple in the first row and remains relatively high due to the influence of the horseshoe vortex by the dimple in the last row. Heat transfer is promoted in front of the 8 mm diameter dimple by the horseshoe vortex. Since the upper part of the 8 mm dimple contacts the upper flat plate, the heat transfer coefficient is relatively low behind the dimple where the flow is weak. In the second and fourth dimples from the left of the second row, since the upper part of the dimple does not contact the upper flat plate and faces the concave portion of the upper flat plate dimple, the heat transfer coefficient is shown to be high throughout the dimple due to the heat transfer promotion by the secondary flow in the concave portion.

Fig. 4 shows a comparison of the pressure losses in the inlet and outlet of the plastic plate heat exchangers. Pressure loss is largest in the corrugate type heat exchanger where the heat transfer surface is complicated with prominences and depressions and the angle of the peaks guiding the flow is set at 45° to the inlet

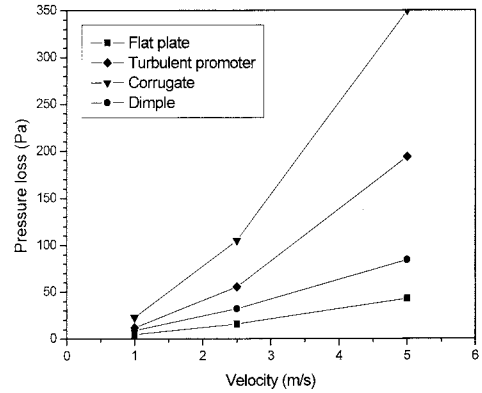


Fig. 4. Comparison of pressure loss of four plastic heat exchanger models.

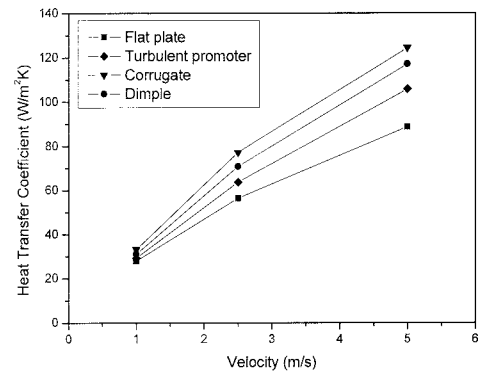


Fig. 5. Comparison of average heat transfer coefficient of four plastic heat exchanger models.

flow. Pressure loss is second largest in the turbulent heat exchanger equipped with a vortex generator and a turbulent promoter. In the dimple heat exchanger equipped with 3 mm and 8 mm diameter hemispherical dimples, pressure loss is slightly higher than that with the flat plate type and lower than that of the turbulent promoter type. In all the four models, pressure loss tends to increase as the velocity increases in the inlet. In the corrugate heat exchanger, the increase rate of pressure loss is noticeably higher than in other types. With the inlet velocity of 5 m/s, the pressure losses of the turbulent promoter, dimple and corrugate types increase by about 350%, 100% and 720% respectively compared to the flat plate type.

Fig. 5 shows a comparison of the average heat transfer coefficients on the heat transfer surface of the plastic plate heat exchangers. Because the corrugate type destroys thermal boundary layer where the lower plate's peaks and the upper plate's valleys meet and makes complex 3-D turbulent flow with as low of

Reynolds number as possible, the average heat transfer coefficient is highest in the corrugate type heat exchanger, second highest in the dimple type heat exchanger and third highest in the turbulent promoter type heat exchanger. The average heat transfer coefficient increases as the inlet velocity increases but, unlike pressure loss, the increase rate decreases as the velocity increases. The heat transfer coefficients of the turbulent promoter type, dimple type and corrugate type are higher by about 20%, 30% and 40% respectively compared to the flat plate type.

Fig. 6 shows a graph comparing the results of experiment for the friction coefficients of the plastic plate heat exchangers with the computational analysis results. The experiment and computational analysis results both show that the friction coefficient is highest in the corrugate type, followed by the turbulent promoter type, dimple type and flat plate type. The test and computational analysis results with the flat plate type are well matched with each other. The computational analysis results with the dimple type show a slightly low distribution. The computational analysis results with the corrugate and turbulent promoter types show a higher distribution than the test results. With the Reynolds number 2700, the friction coefficients of the corrugate, dimple and turbulent promoter types increased by about 900%, 140% and 430% respectively.

Fig. 7 shows a comparison of Nu numbers. The experiment and computational analysis results both show that the Nu number distribution is highest in the corrugate type, followed by the dimple type, turbulent promoter type and flat plate type but present different values. With the Reynolds number 2700, the Nu numbers of the corrugate, dimple and turbulent promoter types increased by about 95%, 80% and 35% respectively.

Comparison of Nusselt numbers, friction factors and their ratios based on equivalent fan power for four types of heat exchanger are given in Fig. 8. The corrugate type produces the best performance in the experimental results, and the dimple type takes the second place. The turbulent promoter type does not show better overall performance than that of the corrugate type and the dimple type, since the turbulent promoters and the ribs contribute to enhance the heat transfer rate more than occurring pressure loss in high Reynolds number. But, in the computational results, the dimple type produces the best performance, because the computational results of friction factor for dimple type is lower than that of the experimental results and the computational results of

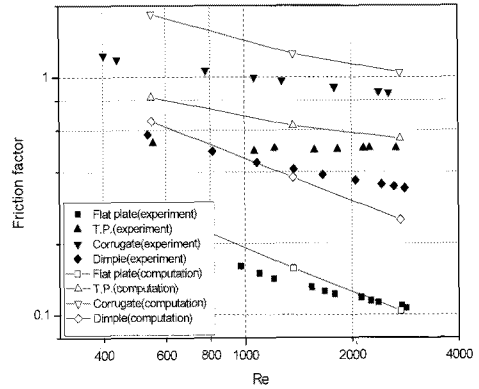


Fig. 6. Comparison of friction factors at various Reynolds numbers.

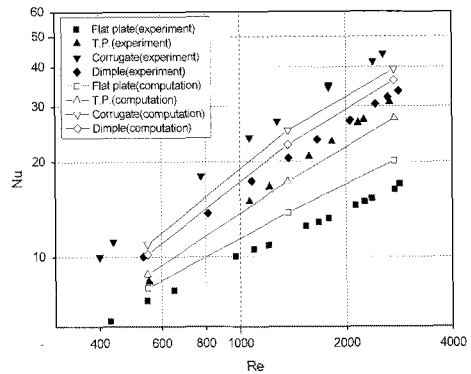


Fig. 7. Comparison of Nusselt numbers at various Reynolds numbers.

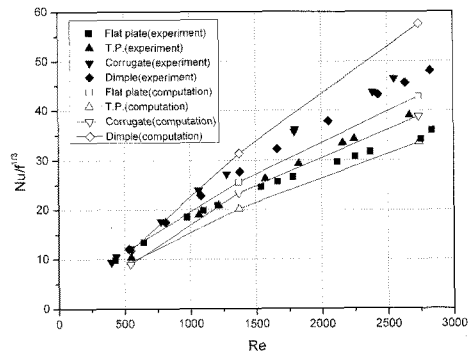


Fig. 8. Comparison of value of the term $Nu/f^{1/3}$ on Reynolds number.

Nusselt number for dimple type is higher than that of experimental results. These comparisons indicate that the corrugate type and the dimple type can be the best design in the plastic plate heat exchangers.

6. Conclusion

The results of computational analysis of the four type plastic plate heat exchangers - the flat plate type, turbulent promoter type, dimple type and corrugate type - are summarized as follows.

- (1) With the Reynolds number 2700, the friction coefficients of the corrugate type, dimple type and turbulent promoter type increased by about 900%, 140% and 430% respectively compared to the flat plate type heat exchanger.
- (2) With the Reynolds number 2700, the Nu numbers of the corrugate type, dimple type and turbulent promoter type increased by about 95%, 80% and 35% respectively compared to the flat plate type heat exchanger.
- (3) The experiment and computational analysis results both show that the friction coefficient is highest in the corrugate type, followed by the turbulent promoter type, dimple type and flat plate type heat exchanger.
- (4) The experiment and computational analysis results both show that the Nu number distribution is highest in the corrugate type, followed by the dimple type, turbulent promoter type and flat plate type heat exchanger. The tendency of numerical simulation results is in good agreement with that of the experimental results.

Acknowledgment

This research is partially supported by the Small and Medium Business Administration and Korea Energy Management Corporation.

References

- [1] Chung, M. H., 2003, A Study on the Heat Recovery Performance of Plastic and Paper Heat Exchanger, Ph. D. dissertation, Chungnam National University, Daejeon, Korea.
- [2] Fiebig, M., Guntermann, T. and Mitra, M. K., 1995, Numerical Analysis of Heat Transfer and Flow Loss in a Parallel Plate Heat Exchanger Element with Longitudinal Vortex Generators as Fins, Trans. of ASME, J. of Heat Transfer, Vol. 117, pp. 1064-1067.
- [3] Choi, S. W., Paik, Y. H., Kang, H. C. and Kim, D. Y., 1997, Calculation of a 2-D Channel Flow with a Dimple, Trans. of KSME(B), Vol. 21, No. 1, pp. 49-56.
- [4] Stasiek, J. A., 1998, Experimental Studies of Heat Transfer and Fluid Across Corrugated-undulated Heat Exchanger Surfaces, Int. J. Heat Mass Transfer, Vol. 41, No. 6-7, pp. 899-914.
- [5] Yoo, S. Y., Chung, M. H., Kim, K. H. and Lee, J. M., 2005, An Experimental Study on the Performance of Plastic Plate Heat Exchanger, Korean Journal of Air-Conditioning and Refrigeration Engineering, Vol. 17, No. 2, pp. 117-124.
- [6] FLUENT6 USER'S GUIDE, 2001, Fluent Inc., New Hampshire, USA.